Analecta Technica Szegedinensia
Vol. 19, No. 1 ISSN 2064-7964 2025

OPTIMIZATION OF OPERATIONAL PARAMETERS TO ENHANCE ULTRAFILTRATION EFFICIENCY USING DAIRY WASTEWATER MODEL

[1,2,*]Aws N. Al-Tayawi, [3]Hajnalka Csott, [4]Zsuzsanna Horváth Hovorka, [5]István Hatos, [3]Zsuzsanna László, [3]Gábor Veréb, [6]Maravic Nikola, [6]Zita Šereš, and [3]Szabolcs Kertész

[1]Doctoral School of Environmental Sciences, University of Szeged, Szeged H-6725, Hungary,
[2]Department of Environmental Technology, Faculty of Environmental Sciences, University of Mosul, Mosul 41002, Iraq,
[3]Department of Biosystems Engineering, Faculty of Engineering, University of Szeged, Szeged H-6725, Hungary,
[4]Department Department of Mechanical Engineering, Faculty of Engineering, University of Szeged, Szeged H-6725, Hungary
[5]Department of Materials Science and Technology, Audi Hungaria Faculty of Automotive Engineering, Széchenyi István University, Győr H-9026, Hungary,
[6]Faculty of Technology Novi Sad, University of Novi Sad, Bulevar Cara Lazara 1, 21000 Novi Sad, Serbia,

*Correspondence e-mail: awsaltayawi@uomosul.edu.iq

Received: 3rd February	*Accepted: 20th March*

ABSTRACT

Ultrafiltration is a key technology for treating dairy wastewater; however, its efficiency is often hindered by critical challenges such as membrane fouling and concentration polarization. To mitigate these issues, one effective approach involves optimizing operational parameters to enhance system performance and longevity. In this study the influence of key operational parameters on the performance of a lab-scale low-pressure ultrafiltration membrane system for treating dairy wastewater model were investigated. The optimization focused on three critical factors: transmembrane pressure (TMP), stirring speed, and membrane molecular weight cut-off (MWCO). Key performance metrics, including permeate flux, membrane retention efficiency, and total, reversible, and irreversible membrane resistances, were analyzed. The results showed that the optimal conditions were identified using a 20 kDa polyethersulfone membrane, with a TMP of 0.3 MPa and a stirring speed of 400 rpm. Statistical analysis was conducted to further refine and validate the optimization of these parameters.

Keywords: Ultrafiltration; Dairy wastewater; Transmembrane pressure; Stirring speed; molecular weight cut-off.

1. INTRODUCTION

The escalating environmental challenges driven by rapid population growth have highlighted the urgent need to protect natural water resources [1,2]. Among the key sectors contributing to this issue is the dairy industry, which consumes significant volumes of water and generates complex wastewater streams, posing substantial management challenges [3,4]. The adoption of advanced, reliable technologies, such as hybrid or combined processes, is essential for the effective treatment of high-organic-content wastewater [5]. In this context, ultrafiltration, a membrane-based separation process, has emerged as a promising solution and is increasingly integrated into industrial and wastewater treatment applications [6].

A major limitation of membrane-based processes is membrane fouling, which is often accompanied by concentration polarization [7–9]. Membrane fouling significantly reduces permeate flux, compromises rejection efficiency, and increases energy consumption [10,11]. It occurs when foulants, including particulate matter, colloidal particles, biomacromolecules, and various organic, inorganic, and biological substances, adhere to the membrane surface or within its pores [12]. This adhesion obstructs or reduces pore size, leading to diminished permeation flux and altered separation efficiency [13,14]. Fouling is categorized as irreversible when foulants block membrane pores, impeding permeate flow, or reversible when a cake layer forms on the membrane surface, increasing overall resistance [15,16]. Fouling consistently reduces membrane performance by decreasing active surface area, shortening membrane lifespan, and increasing operational and replacement costs [17–19].

To address fouling, optimizing operational parameters such as transmembrane pressure, stirring speed, and membrane molecular weight cut-off are critical [20]. Adjusting these parameters influences fouling behavior;

DOI: https://doi.org/10.14232/analecta.2025.1.45-58

for instance, stirring speed is considered essential for maintaining a uniform concentration gradient across the membrane surface, which directly influences the permeate flux. An increase in stirring speed has been shown to enhance the mass transfer of solutes to the membrane surface, thereby reducing concentration polarization and improving the overall filtration rate [21,22]. Moreover, transmembrane pressure (TMP) is another critical parameter that governs the driving force for permeation through the membrane [23]. A higher TMP has the potential to increase the permeate flux; however, it may also result in higher fouling rates, highlighting the necessity of fine-tuning this parameter for specific applications [24,25]. Furthermore, the molecular weight cut-off value of the membrane plays a pivotal role in determining the selectivity of the ultrafiltration process. The selection of membrane cut-off directly affects the separation efficiency of target solutes from the feed solution [26–28]. This study systematically investigates the optimization of key operational parameters to enhance filtration performance in dairy wastewater treatment. Stirring speed, transmembrane pressure, and molecular weight cut-off were optimized using a lab-scale model. Comprehensive statistical analyses, at a significance level of $p<0.005$ and a confidence interval of 0.95, thus helping to confirm the most appropriate choice, were conducted to refine these parameters, providing robust insights into their influence on ultrafiltration efficiency.

2. MATERIALS AND METHODS

2.1 Typical Parameters for Membrane Filters

The performance of a membrane is typically characterized by several key parameters. Filtration efficiency is commonly quantified through permeate flux, as defined by Equation (1) [9,29]. Membrane selectivity is assessed based on retention or rejection rates, expressed mathematically in Equation (2) [30,31]. Additionally, the economic viability of the process can be evaluated in terms of membrane resistance.

In the initial stages of membrane filtration and in distilled water measurements, the resistance is solely due to the hydrodynamic resistance of the membrane. However, in reality, the total resistance (RT) (Equation. 3) is consist of several factors, including membrane resistance (RM) (Equation. 4), the resistance of the polarization layer on the membrane surface (RREV) (Equation. 5), and the resistance caused by fouling of the pores (RIRREV) (Equation. 6). [32–34].

Moreover, transmembrane Pressure Difference was calculated with (Equation. 7) [35,36], Volume Reduction Ratio (VRR) was calculated with (equation. 8) [37,38], and Reynolds Number was calculated with (equation. 9) [39–42].

$$J = \frac{1}{A} \cdot \frac{dV}{dt} \quad [L \cdot m^{-2} \cdot h^{-1}] \tag{1}$$

$$R = \frac{c_f - c_p}{c_f} \cdot 100 \ [\%] \tag{2}$$

$$R_T = R_M + R_{IRREV} + R_{REV} \ [m^{-1}] \tag{3}$$

$$R_M = \left(\frac{TMP}{J_{WB} \cdot \eta_W}\right) \ [m^{-1}] \tag{4}$$

$$R_{REV} = \frac{TMP}{J_{WA} \cdot \eta_W} - R_M - R_{IRREV} \ [m^{-1}] \tag{5}$$

$$R_{IRREV} = \frac{TMP}{J_{WA} \cdot \eta_W} - R_M \ [m^{-1}] \tag{6}$$

$$TMP = \frac{p_{mi} + p_{mo}}{2} - p_0 \ [Pa] \tag{7}$$

$$VRR = \frac{V_f}{V_f - V_p} \tag{8}$$

DOI: https://doi.org/10.14232/analecta.2025.1.45-58

$$N_{Re}=\frac{\rho v d}{\eta} \quad (9)$$

2.2. Wastewater Model Preparation

The model effluent similar to dairy wastewater was freshly prepared before each measurement. Skimmed milk powder (Tutti Kft., Hungary) and anionic detergent (Chemipur Cl80, Szeged, Hungary) were adjusted to concentrations of 5 g L^{-1} and 0.5 g L^{-1}, respectively, using tap water at 25 ° C. This concentration range aligned with the existing literature on the chemical oxygen demand (*COD*) values for average dairy wastewater [43], The recorded average values recorded of the model effluents were as follows: *COD* [mgL^{-1}] 5200, turbidity [NTU] 1150, pH 8.7, and electrical conductivity [mS] 0.89.

2.3. Laboratory Equipment

A static stirred laboratory ultrafiltration system (Merck Millipore, Germany) was utilized. *PES* (polyether sulfone) membranes of various cut-off values (10, 20, and 50 kDa), together offering an effective filtration area of 0.0036 m^2, were used in the apparatus. The transmembrane pressure was managed by the nitrogen gas control of the bottle and a pressure regulator valve. The filter was released through a tube on the bottom plate, maintaining a compression ratio of 2 (*VRR*=2, volumes reduced from 100 ml to 50 ml). Continuous permeate mass measurements were recorded using an electric balance (Kern EW, Germany).

2.4. Laboratory Membrane Filtration Measurements

A fresh preparation of the model dairy wastewater in the specified concentration ratios was used for each measurement. A membrane support, permeate drainage mesh, and *PES* membrane were inserted into the stainless steel bottom of the unit. The glass cylinder wall was placed on the O-ring, followed by the cover, and a membrane wetting process of 30 minutes was started at a low pressure of 0.05 MPa by loading clean water. The flux of the pure membrane permeate was subsequently determined. The remaining water from the unit was removed and 100 ml of the initial freshly homogenized effluent was loaded into the apparatus. The instantaneous mass of the permeate was recorded at given time intervals using the balance software. The stirring speed (n) and pressure (*TMP*) were set and the *VRR* was performed up to twice rate, that is, until 50 mL of filtrate was obtained. When the measurement was complete, the reversible polarization layer was removed from the membrane surface, placed back in the unit, and the run-off time was recorded again. Thus, the irreversible resistance value was calculated later using Equation (6). The initial effluent, concentrate, and permeate were then collected to perform analytical measurements.

Turbidity, conductivity, total dissolved solids (TDS), and chemical oxygen demand (*COD*) were also measured. During the first series of measurements, experiments were carried out with different transmembrane pressures (2 bar and 4 bar), stirring speeds (0 rpm, 200 rpm and 400 rpm) and different cut-off values (10 kDa, 20 kDa and 50 kDa). All possible pairings were combined to obtain the most detailed statistical evaluations (using Statistica), and the optimum was selected based on filtration time, quality, and economy.

2.6. Analytical Instruments

Analytical instruments were used to assess the filtrate, initial model wastewater, and concentrate samples. These instruments included a Thermo Scientific Orion 5-Star Plus Multifunction Benchtop Meter (Thermo Fisher Scientific, Massachusetts, USA) for pH measurement, a Hach 2100N Turbidimeter (Hach Company, Colorado, USA) for turbidity measurements, destructive block Lovibond RD 125 and photometer Lovibond MD 200 (Tintometer Group, Dortmund, Germany) to determine organic matter content through *COD*, and a portable instrument Voltcraft Cond, *TDS*, Salt, KBM-90 (Voltcraft, Hirschau, Germany) to assess *TDS*, conductivity, and salinity.

DOI: https://doi.org/10.14232/analecta.2025.1.45-58

3. RESULTS AND DISCUSSION

3.1. Fluxes

Six measurements were conducted with different membranes pore-size, *TMP* and stirring speed. The initial flux values measured with different pore size membranes ranged from 90-120 $Lm^{-2}h^{-1}$ for the 10 kDa, 100-160 $Lm^{-2}h^{-1}$ for the 20 kDa, and 110-180 $Lm^{-2}h^{-1}$ for the 50 kDa membrane, and were then subject to an intense decrease of 60-70% already up to a *VRR* of 1.05. This decrease was expected, because flow conditions in membrane separation processes are predominantly established at the beginning of filtration due to fouling, and their efficiency and flux values also decrease with time. This was followed by a flattening, converging phase. Very similar responses in flux trends to pressure and changes in stirring rate were observed for membranes of different cut-off values (10-20-50 kDa). The decrease in flux observed with increasing rotational speeds from 200 to 400 rpm for a 50 kDa cut-off membrane is attributed to the effects of shear forces, concentration polarization, and fouling dynamics. At lower speeds, fouling and concentration polarization are mitigated by the action of shear forces. Although an improvement in flux is initially achieved at higher speeds through foulant removal and enhanced mass transfer [44], a reduction in permeate flow is caused by the compaction of fouling layers under excessive shear [45]. Furthermore, membrane properties, such as porosity, are affected by higher shear forces, affecting the filtration performance, as identified in studies on optimal rotational speeds [46]. The time variations of the flux values measured with the 20 kDa cutoff membrane are shown in Fig. 1. It can be observed that at more intense stirring (both at 200 rpm and 400 rpm), the filtration rates were remarkably accelerated, and their flux values were set to values orders of magnitude higher compared to the filtration processes without stirring.

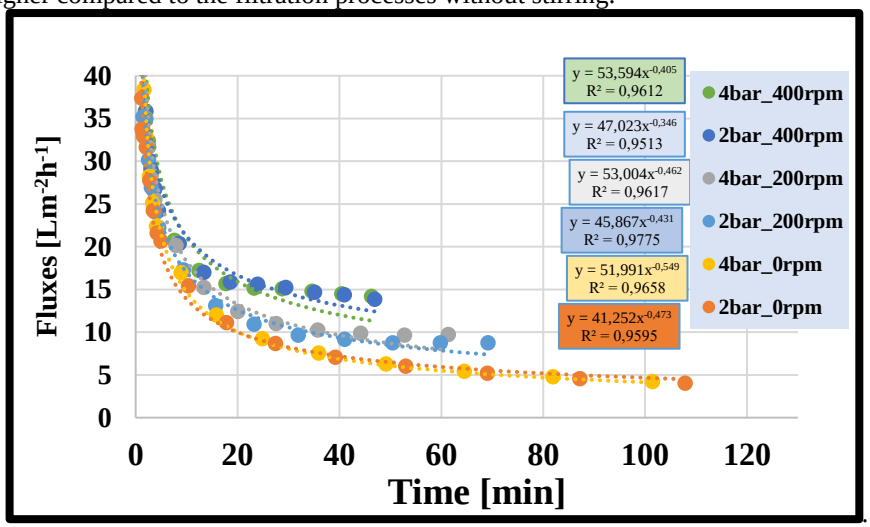

Figure 1. Variation of permeate fluxes as a function of time at different pressures and stirring speeds (*MWCO*=20 kDa; T=25°C).

It is essential to determine the type of flow within the unit. Fig.2 presents the Reynolds number values for different stirring speeds. At speeds of 200, 300, and 400 rpm, the Reynolds numbers are 4108, 6162, and 8215, respectively, indicating turbulent flow. At a speed of 100 rpm, a transitional flow is observed. Due to increasing the stirring speed the turbulent flow will dominate, resulting in increasing the permeate fluxes [47,48].

DOI: https://doi.org/10.14232/analecta.2025.1.45-58

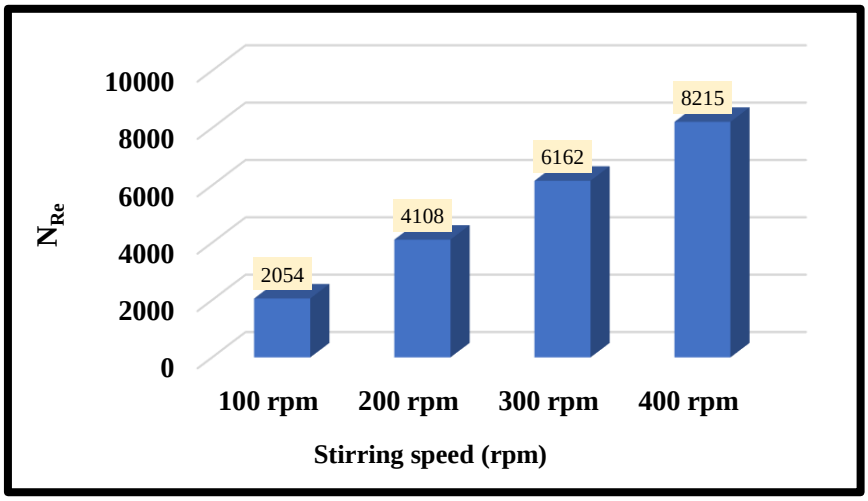

Figure 2. Reynolds number values as a result of increasing stirring speed.

For more efficient analysis, a linear line/curve was also fitted to the initial flux values in the work. It was found that due to the flow conditions at the beginning of the filtrations and the intense membrane fouling, it is indeed linearly decreasing in all cases. In fact, it was observed that the extent of this intense decrease was largely determined by the overall duration of the filtration and the magnitude of the average flux values. The steeper the slope of the linear curve fitted to the initial flux values where the data were measured up to 5 g of runoff, the stronger the magnitude of the initial flux drop, thus reaching the converging phase sooner. The effect of pressure and membrane pore size increased this slope, while the presence of stirring did not change the magnitude of the initial flux drop to any great extent. Compared to the 10 kDa membrane cutoff, the average fluxes of the 20 and 50 kDa membranes were higher. As pressure increased, the average flux values also increased by approximately 25%, and the filtration time at 4 bar was significantly reduced compared to 2 bar. However, it should be noted that the initial flux decrease was also more pronounced. The average flux value also improved with the presence and then the stirring speed. Lemmer *et al.* (2020) [47] in were shown similar trend of permeate flux increase with increasing stirring speed. The average flux increases are illustrated in Table 1 below:

Table 1. Variation of average flux values with pressure, stirring speed, and membrane pore size.

Measurements	Average flux values [L m^{-2} h^{-1}]		
	10 kDa	20 kDa	50 kDa
2 bar, 0 rpm	36.02	37.33	39.43
2 bar, 200 rpm	38.25	39.74	41.1
2 bar, 400 rpm	40.41	41.21	39.97
4 bar, 0 rpm	45.39	46.91	44.31
4 bar, 200 rpm	48.42	51.64	51.82
4 bar, 400 rpm	48.44	51.88	51.07

The trends in the measured data and the calculated data according to Equation (1) were analyzed using ANOVA. Calculations were performed with the Statistica program. The results of ANOVA for the flux are illustrated in Fig. 3. To show the differences caused by changing the parameters, we plotted the average values with the confidence intervals at the 0.95 level. A statistically significant difference ($p<0.05$) was observed in the average fluxes of the 20 kDa and 50 kDa membranes compared to the cutoff value of the 10

DOI: https://doi.org/10.14232/analecta.2025.1.45-58

kDa membrane. Similarly, increasing pressure and stirring speed also had statistically significant effects. The average flux values for filtration at 2 bar compared to filtration at 4 bar, and increasing stirring speed from 0 rpm to 200 rpm or from 0 rpm to 400 rpm, all resulted in statistically significant improvements. Furthermore, increasing pressure led to a significant difference in the slopes of the initial flux drop. The slope decreased by approximately 60 units at a pressure of 4 bar compared to that at 2 bar.

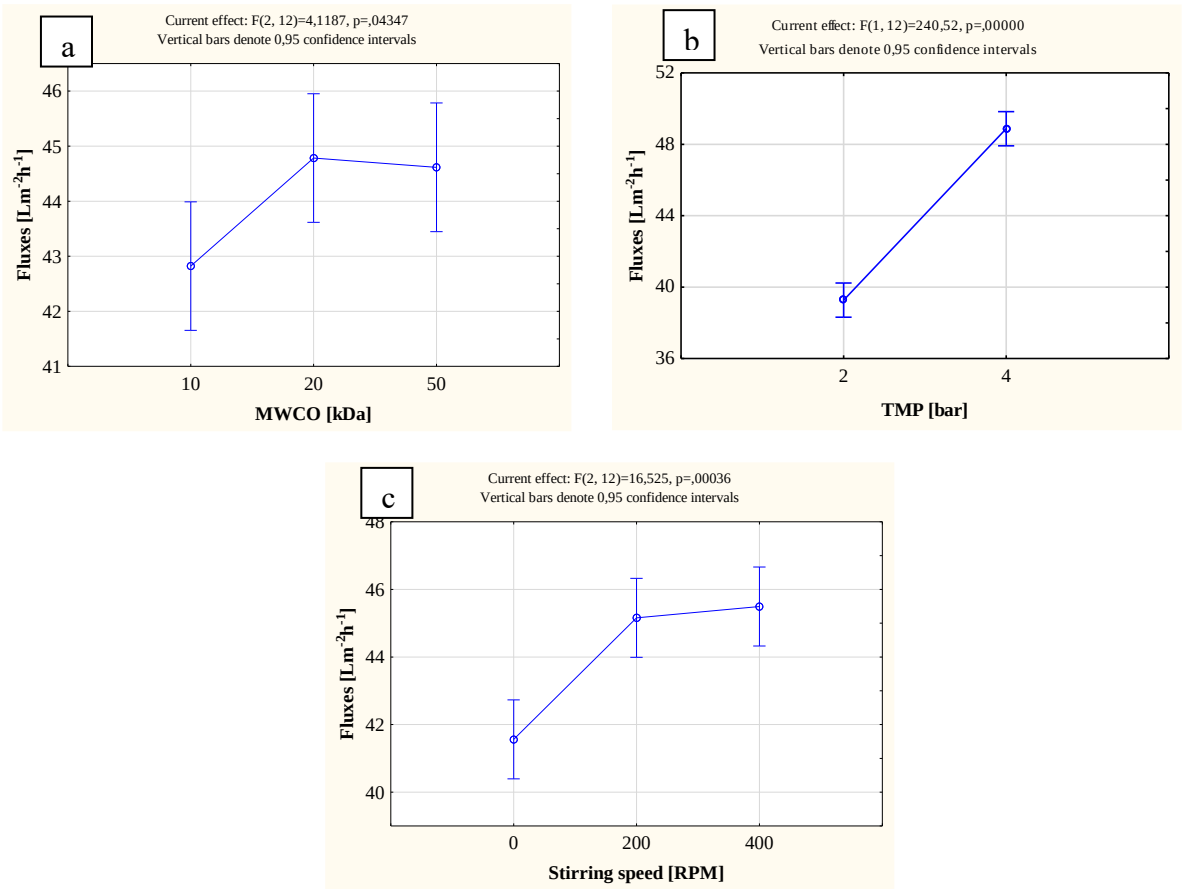

Figure 3. Results of ANOVA: average flux values as a function of the membrane cutoff value (a), pressure (b), and stirring speed (c).

3.2. Membrane Retention

The retention values of the membranes for turbidity, total dissolved solids, salts, and organic matter content were determined. No large differences in turbidity and conductivity retention were observed when the parameters were varied, whereas for organic matter retention, the differences were more significant. The retention of turbidity exceeded 99.9% in all cases, indicating that most of the turbidity-related substances were retained, even by the membrane with the highest cutoff value of 50 kDa. In general, high suspended solids reduction is achieved through ultrafiltration, based on the pore size of the membrane relative to the size of the suspended solids particles. The values for total salinity retention were low, averaging around 2-10%, since most of the ions were allowed to pass through the ultrafiltration membranes.

Fig. 4 shows the percentage change in retention values with increasing pressure and varying stirring speed for ultrafiltration with a 10 kDa cutoff membrane. From the results, it was observed that the retention value

DOI: https://doi.org/10.14232/analecta.2025.1.45-58

of organic matter given in *COD* was not significantly affected by the pressure with the 10 kDa cutoff membrane but was improved by stirring at 200 rpm and 400 rpm. It should be noted that a trend of 5% variation was observed, indicating that changing the operating parameters does not significantly improve retention percentages. For the 20 kDa cutoff value (Fig.5), the pressure magnitude slightly reduced the retention percentage, while the stirring magnitude contributed significantly. Similarly, for the 50 kDa cutoff membrane (Fig.6), both increasing the pressure magnitude and the stirring speed improved the organic matter retention values, although by only 15% overall.

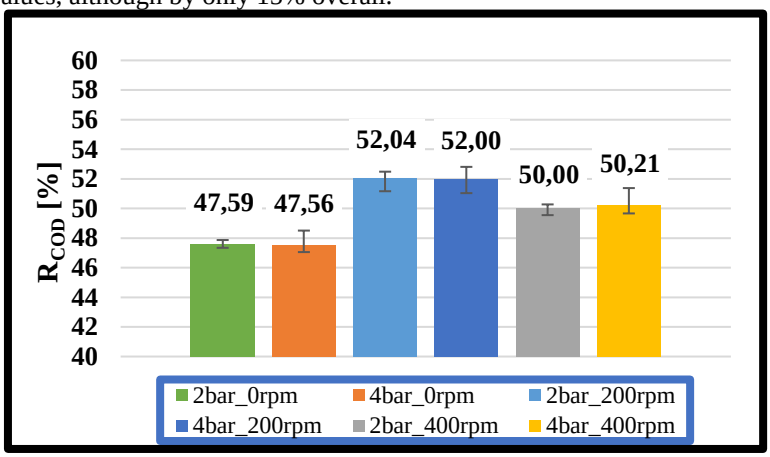

Figure 4. Retention values of the 10 kDa membrane as a function of organic matter content, based on *COD* measurements (T=25°C).

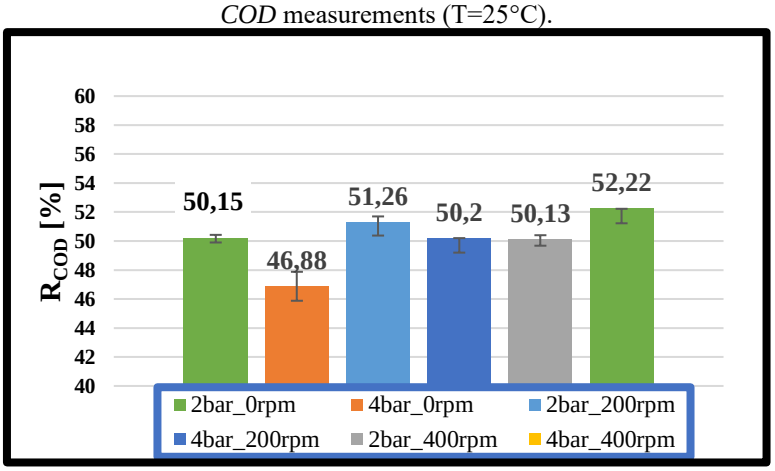

Figure 5. Retention values of the 20 kDa membrane as a function of organic matter content, based on *COD* measurements (T=25°C).

DOI: https://doi.org/10.14232/analecta.2025.1.45-58

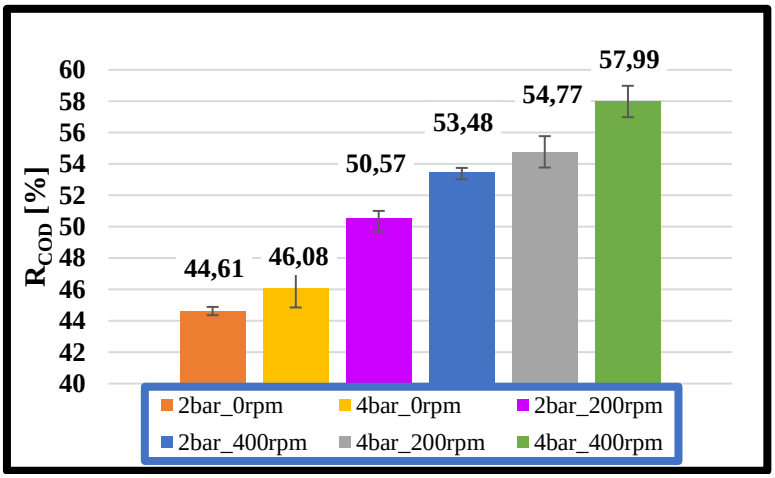

Figure 6. Retention values of the 50 kDa membrane as a function of organic matter content, based on *COD* measurements (T=25°C).

The results of ANOVA also confirm that the effect of the stirring speed on the retention values was found to be positive with a significant difference. However, the increase from 200 to 400 rpm did not yield a significant improvement; only a small enhancement (considering the confidence interval at the 0.95 level) is depicted in Fig. 7.

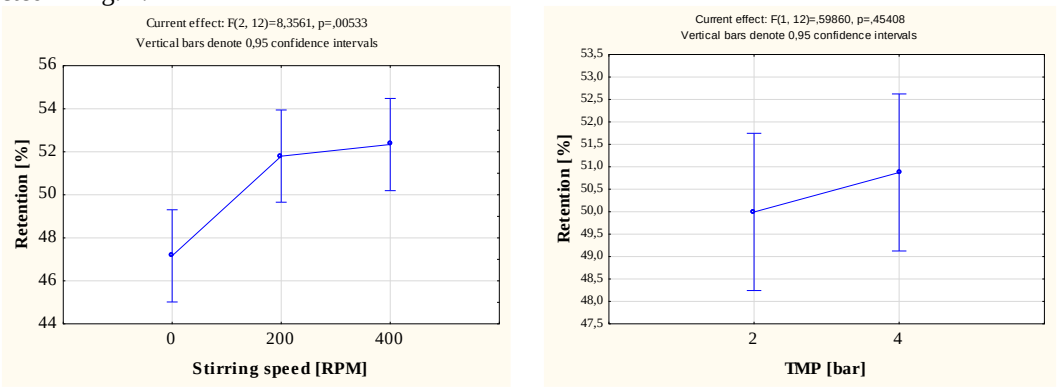

Figure 7. Results of ANOVA: average retention values as a function of stirring speed (a) and pressure (b).

3.3. Resistances-in-Series Model

The resistance values such as membrane, irreversible, reversible, and total resistances were determined using Equations (5), (6), (7), (8), respectively. Variation in the membrane cutoff value did not lead to significant differences in the trend of total resistance values. Consequently, the results presented in Fig. 8. are based on a single membrane with a cutoff value of 20 kDa. It was observed that the total resistance values decreased with increasing stirring speed, while they increased significantly with higher pressure. Specifically, a 22% reduction in total resistance was observed at a stirring speed of 200 rpm compared to the resistance measured at 2 bar pressure and 0 rpm, and a 64% reduction was observed at 400 rpm under the same pressure conditions. When comparing the total resistance at 4 bar pressure and without stirring, improvements of 38% at 200 rpm and 61% at 400 rpm were recorded. In the absence of stirring, increasing the pressure from 2 bar to 4 bar resulted in a 120% increase in total resistance, which is 75% higher compared to resistance at 200 rpm and 40% higher compared to 400 rpm. The smallest improvement, 38%, was achieved on resistance at 4 bar with 0 rpm and 200 rpm, while the largest improvement, 84%, was observed at 2 bar and 0 rpm. Fig.

DOI: https://doi.org/10.14232/analecta.2025.1.45-58

8. shows that the total resistance during filtration at 4 bar and 0 rpm is nearly six times greater than that at 2 bar and 400 rpm. Similar trends, with slight deviations, were seen at lower pressures without stirring compared to higher pressures at high stirring speeds. The positive impact of the increase in stirring speed was found to be less significant than the negative impact of the increase in pressure, although the detrimental effect of higher pressure was somewhat mitigated by the increase in stirring speed.

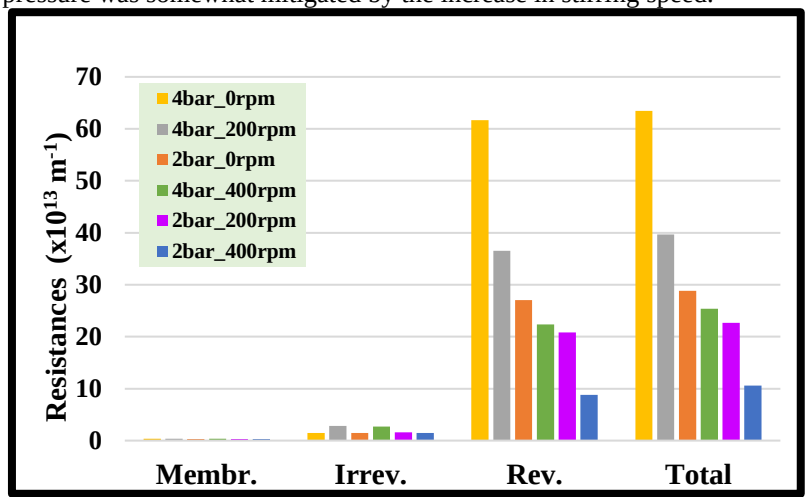

Figure 8. Changes in resistance values at different stirring speeds and pressures with the 20 kDa membrane (T=25°C).

Of the resistance values, the reversible resistance was clearly identified as the dominant one, representing 80-90% of the total resistance. This dominance can be advantageous in terms of the positive effects of changes in the cleaning and flow conditions. At cutoff values of 20 kDa and 10 kDa, similar results were obtained for total resistance, with pressure values increasing considerably and stirring speed decreasing it. On the contrary, for the 50 kDa membrane, a slight decrease in reversible resistance as a percentage was observed compared to the other cut-off values, resulting in increased irreversible values. This indicates more fouling in the membrane pores, which would not respond to simple surface washing/rinsing. Additionally, it can be noted that minimally higher irreversible fouling is observed for membranes with higher cutoff values. ANOVA revealed that there were no significant differences in resistance reduction with changes in the pore size of the membrane. However, for the total resistance value, significant differences were observed when increasing the pressure from 2 bar to 4 bar and increasing the stirring speed from 0 rpm to 200 rpm, and then from 200 rpm to 400 rpm. These results are illustrated in Fig. 9, considering the 0.95 confidence interval level.

DOI: https://doi.org/10.14232/analecta.2025.1.45-58

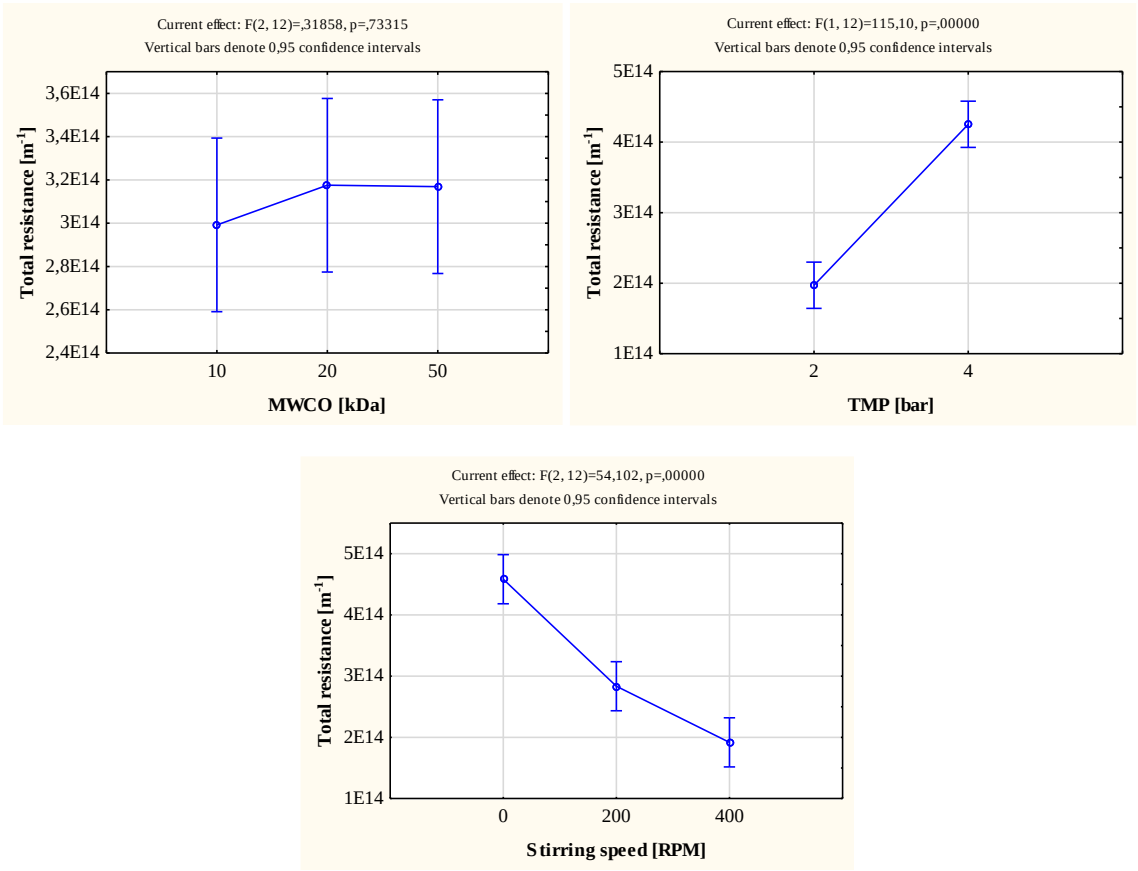

Figure 9. Result of ANOVA: average of total resistance values as a function of membrane cutoff value (a), pressure (b), and stirring speed (c).

By comparing the measurements and the statistical analysis, it can be concluded that increasing the stirring speed strongly reduced (i.e. improved) the total resistances, while the magnitude of the applied pressure did not significantly decrease and the cut-off values did not significantly affect the total resistance value and its percentage distribution. The conclusion of the study of the operational parameters indicates that the flux values increased with increasing the cutoff value of the membrane and also with increasing the stirring speed and pressure. Organic matter retention was greatly improved by stirring, but the other parameters were not significantly altered. The total resistance was not significantly affected by the cutoff values, while the stirring speed decreased, i.e., improved it, and the pressure increased, i.e., worsened it.

4. CONCLUSIONS

This study investigated the impact of optimizing operational parameters on ultrafiltration performance using a laboratory-scale membrane separation unit and a dairy model effluent. A comprehensive analysis was conducted to evaluate flow dynamics and ultrafiltration efficiency by systematically varying key operating parameters, including transmembrane pressure, stirring speed, and membrane molecular weight cut-off. Experimental results encompassed a broad range of filtration conditions to determine optimal performance settings. The findings revealed that increasing pressure and stirring speed significantly enhanced average

DOI: https://doi.org/10.14232/analecta.2025.1.45-58

flux, while retention values remained relatively stable. The optimal operating conditions were identified as a 20 kDa membrane, a transmembrane pressure of 3 bar, and a stirring speed of 400 rpm.

AKMOWLEDGEMENT

This study was supported by the 142414 FK and 2022-1.2.6-TÉT-IPARI-TR-2022-00011 grants from the National Research, Development and Innovation Office (NKFI), Hungary. Aws N. Al-Tayawi acknowledges the financial support provided through the Ministry of Culture and Innovation Research Fellowship Program, funded by the National Fund for Research, Development and Innovation (grant number EKÖP-24-3-SZTE-476).

ABBREVIATIONS

TMP	Transmembrane pressure [Pa]
RT	Total resistance [m–1]
RM	Membrane resistance [m–1]
RIRR	Irreversible resistance [m–1]
RREV	Reversible resistance [m–1]
A	Membrane surface area [m2]
J	Flux [L m–2 h–1]
V	Permeate volume [m3]
t	Filtration time [s]
R	Retention [%]
CF	Concentration of the feed [mg L–1]
CP	Concentration of the permeate [mg L–1]
MWCO	Molecular weight cut-off [kDa]
pmi	Module inlet pressure value [Pa]
pmo	Module outlet pressure value [Pa]
p0	The pressure on the permeate side [Pa]
VRR	Volume Reduction Ratio [-]
Vf	Volume of feed [m3]
Vp	Volume of permeate [m3]
JWB	The initial water flux before filtration [L m–2 h–1]
ηw	Water viscosity at 25°C [Pa.s]
JWA	Water flux of the membrane after filtration [L m–2 h–1],
ηW	The dynamic viscosity of water at 25 °C [Pa.s]
Re	Reynolds number [-]
ρ	The solution density [kg m–3]
υ	Velocity [m s-1]
d	Diameter of the magnetic stirrer [m]
η	Solution's viscosity [Pa.s]
TDS	Total dissolved solids
COD	Chemical oxygen demand
PES	Polyethersulfone

REFERENCES

1. Bănăduc, D.; Simić, V.; Cianfaglione, K.; Barinova, S.; Afanasyev, S.; Öktener, A.; McCall, G.; Simić, S.; Curtean-Bănăduc, A. Freshwater as a Sustainable Resource and Generator of Secondary Resources in the 21st Century: Stressors, Threats, Risks,

Management and Protection Strategies, and Conservation Approaches. *Int. J. Environ. Res. Public Health* **2022**, *19*, 16570.
2. Mondal, S.; Palit, D. Challenges in Natural Resource Management for Ecological Sustainability. In *Natural Resources Conservation and Advances for Sustainability*; Elsevier, 2022; pp. 29–59.
3. Grout, L.; Baker, M.G.; French, N.; Hales, S. A Review of Potential Public Health Impacts Associated with the Global Dairy Sector. *GeoHealth* **2020**, *4*, e2019GH000213.
4. Bansal, A.; Kumar, A. Exploring Challenges in Effective Wastewater Treatment for Dairy Industries. In *Sustainability of Water Resources: Impacts and Management*; Springer, 2022; pp. 237–247.
5. Vlotman, D.E.; Key, D.; Bladergroen, B.J. Technological Advances in Winery Wastewater Treatment: A Comprehensive Review. *South African J. Enol. Vitic.* **2022**, *43*, 58–80.
6. Miao, R.; Ma, B.; Li, P.; Wang, P.; Wang, L.; Li, X. Mitigation Mechanism of Ozonation in the Casein Fouling of Ultrafiltration Membranes: Possible Application in Dairy Wastewater Treatment. *J. Memb. Sci.* **2021**, *629*, 119307.
7. Liao, Y.; Bokhary, A.; Maleki, E.; Liao, B. A Review of Membrane Fouling and Its Control in Algal-Related Membrane Processes. *Bioresour. Technol.* **2018**, *264*, 343–358.
8. Reig, M.; Vecino, X.; Cortina, J.L. Use of Membrane Technologies in Dairy Industry: An Overview. *Foods* **2021**, *10*, 2768.
9. Field, R.W.; Wu, J.J. Permeate Flux in Ultrafiltration Processes—Understandings and Misunderstandings. *Membranes (Basel).* **2022**, *12*, 187.
10. Goh, P.S.; Lau, W.J.; Othman, M.H.D.; Ismail, A.F. Membrane Fouling in Desalination and Its Mitigation Strategies. *Desalination* **2018**, *425*, 130–155.
11. Nthunya, L.N.; Bopape, M.F.; Mahlangu, O.T.; Mamba, B.B.; Van der Bruggen, B.; Quist-Jensen, C.A.; Richards, H. Fouling, Performance and Cost Analysis of Membrane-Based Water Desalination Technologies: A Critical Review. *J. Environ. Manage.* **2022**, *301*, 113922.
12. Abu-Zurayk, R.; Alnairat, N.; Khalaf, A.; Ibrahim, A.A.; Halaweh, G. Cellulose Acetate Membranes: Fouling Types and Antifouling Strategies—A Brief Review. *Processes* **2023**, *11*, 489.
13. Lan, Y.; Serrano, K.G.; Coetsier, C.; Causserand, C. Fouling Control Using Critical, Threshold and Limiting Fluxes Concepts for Cross-Flow NF of a Complex Matrix: Membrane BioReactor Effluent. *J. Memb. Sci.* **2017**, *524*, 288–298, doi:10.1016/j.memsci.2016.11.001.
14. Warsinger, D.M.; Swaminathan, J.; Guillén-Burrieza, E.; Arafat, H.A.; Lienhard, J.H. Scaling and Fouling in Membrane Distillation for Desalination Applications: A Review. *Desalination* **2015**, *356*, 294–313, doi:10.1016/j.desal.2014.06.031.
15. Qrenawi, L.I.; Abuhabib, A.A. A Review on Sources, Types, Mechanisms, Characteristics, Impacts and Control Strategies of Fouling in RO Membrane Systems. *Desalin. Water Treat* **2020**, *208*, 43–69.
16. Saffarimiandoab, F.; Gul, B.Y.; Tasdemir, R.S.; Ilter, S.E.; Unal, S.; Tunaboylu, B.; Menceloglu, Y.Z.; Koyuncu, İ. A Review on Membrane Fouling: Membrane Modification. *Desalin. Water Treat* **2021**, *216*, 47–70.
17. Rajendran, D.S.; Devi, E.G.; Subikshaa, V.S.; Sethi, P.; Patil, A.; Chakraborty, A.; Venkataraman, S.; Kumar, V.V. Recent Advances in Various Cleaning Strategies to Control

DOI: https://doi.org/10.14232/analecta.2025.1.45-58

Membrane Fouling: A Comprehensive Review. *Clean Technol. Environ. Policy* **2024**, 1–16.
18. Zhao, Y.; Zhou, Z.; Liu, C.; Li, X.; Wang, T.; Qu, F. Ultrafiltration Membrane Fouling Control Caused by Extracellular Organic Matter Extracted from Microcystis Aeruginosa: Role of Visible Light Pre-Photocatalysis and Membrane Characteristics. *J. Memb. Sci.* **2025**, *717*, 123613.
19. Latif, E.F.; Elmaadawy, K. Overcoming Fouling Challenges in Ultrafiltration for Drinking Water Treatment. *Eng. Res. Express* **2024**, *6*, 42101.
20. Wang, L.; Wang, X.; Fukushi, K. Effects of Operational Conditions on Ultrafiltration Membrane Fouling. *Desalination* **2008**, *229*, 181–191.
21. Liu, J.; Yin, M.; Wang, M.; Zhang, X.; Ge, B.; Liu, S.; Lu, J.; Cui, Z. A Novel Membrane Based Process to Isolate Photosystem-I Membrane Complex From Spinach. *Photosynth. Res.* **2011**, *107*, 187–193, doi:10.1007/s11120-011-9625-5.
22. Liu, Y.; Wang, Z.; Xu, M.; Qi, F.; Li, C.; Sun, D.; Nan, J.; Li, W.; Guan, X.; Ikhlaq, A. Unveiling the Role of Cake Layer in Coagulation-Ultrafiltration on Membrane Fouling and Emerging Application as Dynamic Membrane before Ultrafiltration. *Sep. Purif. Technol.* **2024**, *350*, 127932.
23. Mwanga, N.; Wang, X.; Li, P.; Liu, Y.; Xia, S.; Yin, D.; Rui, M.; Ye, Y. Effect of Micro and Nanobubble Size and Concentration on Membrane Fouling: Strategies for Energy-Saving and Ultrafiltration Efficiency Enhancement. *Desalination* **2024**, *587*, 117929.
24. Al-Tayawi, A.N.; Csott, H.; Lennert, J.R.; Hovorka, Z.H.; László, Z.; Hodúr, C.; Kertész, S. Optimization of Ultrafiltration Parameters in a Laboratory-Scale Unit Using Dairy Model for Membrane Fouling Mitigation. In Proceedings of the Book of Abstracts from the 10th International Scientific Conference on Advances in Mechanical Engineering (ISCAME 2024); Trans Tech Publications Ltd, 2024; Vol. 8, pp. 18–20.
25. John, H. Optimization of Process Parameters for the Production of Soy Protein by Ultrafiltration Using ANN. *J. Food Process. Preserv.* **2024**, *2024*, 1–10, doi:10.1155/2024/5535413.
26. Chan, M.K.; Tan, S.J.; Yeow, A.T.H.; Ng, S.C.; Lau, W.J. Zeolite-Based Poly (Vinylidene Fluoride) Ultrafiltration Membrane: Characterization and Molecular Weight Cut-Off Estimation with Support Vector Regression Modelling. *Membranes (Basel).* **2024**, *14*, 91.
27. Wang, F.; Tarabara, V. V. Pore Blocking Mechanisms during Early Stages of Membrane Fouling by Colloids. *J. Colloid Interface Sci.* **2008**, *328*, 464–469, doi:10.1016/j.jcis.2008.09.028.
28. Li, C.; Ma, Y.; Li, H.; Peng, G. A Convenient Method for the Determination of Molecular Weight Cut-off of Ultrafiltration Membranes. *Chinese J. Chem. Eng.* **2017**, *25*, 62–67.
29. Quezada, C.; Estay, H.; Cassano, A.; Troncoso, E.; Ruby-Figueroa, R. Prediction of Permeate Flux in Ultrafiltration Processes: A Review of Modeling Approaches. *Membranes (Basel).* **2021**, *11*, 368.
30. Lakra, R.; Choudhury, S.; Basu, S. Recovery of Protein and Carbohydrate from Dairy Wastewater Using Ultrafiltration and Forward Osmosis Processes. *Mater. Today Proc.* **2021**, *47*, 1400–1403.
31. Zhang, B.; Feng, X. Assessment of Pervaporative Concentration of Dairy Solutions vs Ultrafiltration, Nanofiltration and Reverse Osmosis. *Sep. Purif. Technol.* **2022**, *292*, 120990.

DOI: https://doi.org/10.14232/analecta.2025.1.45-58

32. Tarapata, J.; Maciejczyk, M.; Zulewska, J. Microfiltration of Buttermilk: Partitioning of Proteins and Modelling Using a Resistance-in-Series Model. *Int. Dairy J.* **2022**, *134*, 105445.
33. Di Bella, G.; Di Trapani, D. A Brief Review on the Resistance-in-Series Model in Membrane Bioreactors (MBRs). *Membranes (Basel).* **2019**, *9*, 24.
34. Tarapata, J.; Dybowska, B.E.; Zulewska, J. Evaluation of Fouling during Ultrafiltration Process of Acid and Sweet Whey. *J. Food Eng.* **2022**, *328*, 111059.
35. Vincent-Vela, M.-C.; Cuartas-Uribe, B.; Álvarez-Blanco, S.; Lora-García, J. Analysis of an Ultrafiltration Model: Influence of Operational Conditions. *Desalination* **2012**, *284*, 14–21.
36. Boyd, C.C.; Duranceau, S.J. Evaluation of Ultrafiltration Process Fouling Using a Novel Transmembrane Pressure (TMP) Balance Approach. *J. Memb. Sci.* **2013**, *446*, 456–464.
37. Kertész, S.; László*, Z.; Forgács, E.; Szabó, G.; Hodúr, C. Dairy Wastewater Purification by Vibratory Shear Enhanced Processing. *Desalin. Water Treat.* **2011**, *35*, 195–201.
38. Chen, Z.; Luo, J.; Wang, Y.; Cao, W.; Qi, B.; Wan, Y. A Novel Membrane-Based Integrated Process for Fractionation and Reclamation of Dairy Wastewater. *Chem. Eng. J.* **2017**, *313*, 1061–1070.
39. Kumar, A.; Panda, U. Microfluidics-Based Devices and Their Role on Point-of-Care Testing. In *Biosensor Based Advanced Cancer Diagnostics*; Elsevier, 2022; pp. 197–224.
40. Whittlesey, R. Vertical Axis Wind Turbines: Farm and Turbine Design. In *Wind Energy Engineering*; Elsevier, 2017; pp. 185–202.
41. Ellenberger, J.P. Chapter 4 - Piping and Pipeline Sizing, Friction Losses, and Flow Calculations. In; Ellenberger, J.P.B.T.-P. and P.C.M. (Second E., Ed.; Butterworth-Heinemann: Boston, 2014; pp. 33–54 ISBN 978-0-12-416747-6.
42. Ghassemi, M.; Shahidian, A. Chapter 4 - Fluid Mechanics. In; Ghassemi, M., Shahidian, A.B.T.-N. and B.H.T. and F.F., Eds.; Academic Press: Oxford, 2017; pp. 57–87 ISBN 978-0-12-803779-9.
43. Shete, B.S.; Shinkar, N.P. Dairy Industry Wastewater Sources, Characteristics & Its Effects on Environment. *Int. J. Curr. Eng. Technol.* **2013**, *3*, 1611–1615.
44. Yu, H.; Huang, W.; Liu, H.; Liang, T.; Chi, N.; Chu, H.; Dong, B. Application of Coagulation–Membrane Rotation to Improve Ultrafiltration Performance in Drinking Water Treatment. *Membranes (Basel).* **2021**, *11*, 643, doi:10.3390/membranes11080643.
45. Igder, A.; Cai, W.; Luo, X.; Al-Antaki, A.H.M.; Vimalanathan, K.; Keshavarz, A.; Nosrati, A.; Raston, C.L. Vortex-Fluidic-Mediated Fabrication of Polysulfone Ultrafiltration Membranes Incorporating Graphene Oxide. *Acs Appl. Polym. Mater.* **2022**, *4*, 4131–4143, doi:10.1021/acsapm.2c00109.
46. Takata, K.; Tanida, K. Effect of UF Membrane Rotation on Filtration Performance Using High Concentration Latex Emulsion Solution. *Membranes (Basel).* **2022**, *12*, 422, doi:10.3390/membranes12040422.
47. Lemmer, B.; Jákói, Z.; Gulyás, N.; Kertész, S.; Beszédes, S.; László, Z.; Hodúr, C. The Effect of Sonication and Stirring on Ultrafiltration of Fermentation Broth. *Environ. Prot. Eng.* **2020**, *46*.
48. Cassano, A.; Conidi, C.; Tasselli, F. Clarification of Pomegranate Juice (<i>Punica Granatum</I> L.) by Hollow Fibre Membranes: Analyses of Membrane Fouling and Performance. *J. Chem. Technol. Biotechnol.* **2014**, *90*, 859–866, doi:10.1002/jctb.4381.

DOI: https://doi.org/10.14232/analecta.2025.1.45-58